Table 1: HHV of Ethanol, *i*-Pentanol, and Gasoline

Compound	Ethanol [1]	*i*-Pentanol [1]	Gasoline [2]
HHV [MJ/kg]	29.67	37.73	48.46

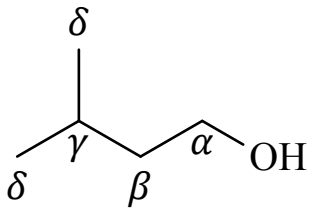

Figure 1: Skeletal structure of *i*-pentanol

0.1 Structure of *i*-Pentanol

i-Pentanol (3-methyl-1-butanol) is a five-carbon alcohol whose skeletal structure is shown in Fig. 1. The carbon atoms in Fig. 1 are labeled according to their distance from the hydroxyl moeity, with α being the closest and δ being the farthest. The Greek letter notation will be used to refer to the carbon-centered radicals in Sec. 0.5. *i*-Pentanol can be produced biologically [3], and offers several similar advantages as the butanol isomers compared to ethanol. Table 1 compares the HHV of ethanol, *i*-pentanol, and gasoline.

0.2 Procedures

Experiments for *i*-pentanol in the RCM have been performed at the conditions listed in Table 2. Homogeneous fuel and air pre-mixtures are prepared in an approximately 17 L mixing tank. The mixing tank and all tubes and manifolds connecting the tank with the RCM are heated, allowing the study of relatively low vapor pressure fuels. The initial temperature is set above the saturation temperature of *i*-pentanol for each mixture studied. The mixing tank is equipped with a magnetic stirrer to ensure complete homogeneity of the mixture.

Prior to mixture preparation, the mixing tank is vacuumed to less than 1 torr, whereupon liquid fuel (*i*-pentanol, Sigma-Aldrich, 99.6 % purity) is injected by a syringe through a septum. The syringe is massed before and after the injection, with the difference being the amount of fuel in the

Table 2: *i*-pentanol Experimental Conditions

Reactant (Purity)			Equivalence Ratio ϕ	Compressed Pressure P_C (bar)
i-pentanol (99.6 %)	O_2 (99.994 %)	N_2 (99.999 %)		
Mole Percentage				
2.41	20.50	77.09	1.0	40
1.22	20.75	78.03	0.5	40
4.71	20.01	75.27	2.0	40

mixing tank. Based on this mass, required proportions of the gaseous oxidizer (O2, 99.994 % purity, N2, 99.999 % purity) are calculated. The gases are added to the mixing tank sequentially at room temperature and the total pressure is monitored to ensure that the proper mixture concentrations are attained. Finally, the heaters and stirring vane are switched on and the system is allowed approximately 1.5 h to reach steady state.

0.3 Model Improvements

Through collaboration with researchers at Lawrence Livermore National Laboratory, many improvements to the chemical kinetic model for *i*-pentanol were made relative to the work of Tsujimura et al. [4]. Some of the major improvements are highlighted below; see the article for more detail [5].

1. The model was restructured based on work with C_4 and C_5 alcohols [6, 7]
2. The most stable conformers of *i*-pentanol were calculated using quantum chemistry software
3. The BDEs of the of the C-C, C-H, C-O, and O-H bonds were calculated using quantum chemistry software
4. The model includes the Waddington pathway shown to be important in low-temperature decomposition of *i*-pentanol by Welz et al. [8]

5. New reaction pathways were added based on the work of Welz et al. [8, 9], including the unconventional water-elimination pathway discussed in Welz et al. [9]

Moreover, the following data sets from the literature and presented in the work of Sarathy et al. [5] were used to validate the newly updated model, in addition to the new data at $P_C = 40$ bar presented here.

1. Ignition delays measured in a ST and an RCM[4, 10]
2. JSR species data [11]
3. New ignition delays measured in STs [5]
4. New JSR species data [5]
5. New flame speed and flame extinction measurements [5]

0.4 Experimental & Modeling Results

The experimental ignition delays measured in the RCM are shown in Figs. 2, 3, and 4, along with ignition delays measured in the ST and comparison with the model simulations. There is no $\phi = 2.0$ data set for 7 atm because no conditions at which ignition occurred could be found. In Figs. 2–4, solid lines represent adiabatic, constant volume simulations, and dashed lines represent volume-profile simulations.

At 7 atm (Fig. 2), the high-temperature ignition delays measured in the ST are generally predicted to within a factor of 1.5. The RCM experiments are also well predicted at low temperature—within a factor of 2—but the disagreement grows to approximately a factor of 4 in the intermediate temperature regime. At 20 atm (Fig. 3), the high-temperature ignition delays are well predicted, including capturing the equivalence ratio sensitivity of the ignition delays. The ignition delays measured in the RCM are fairly well predicted at the lean and stoichiometric conditions, but are over-predicted at the rich condition.

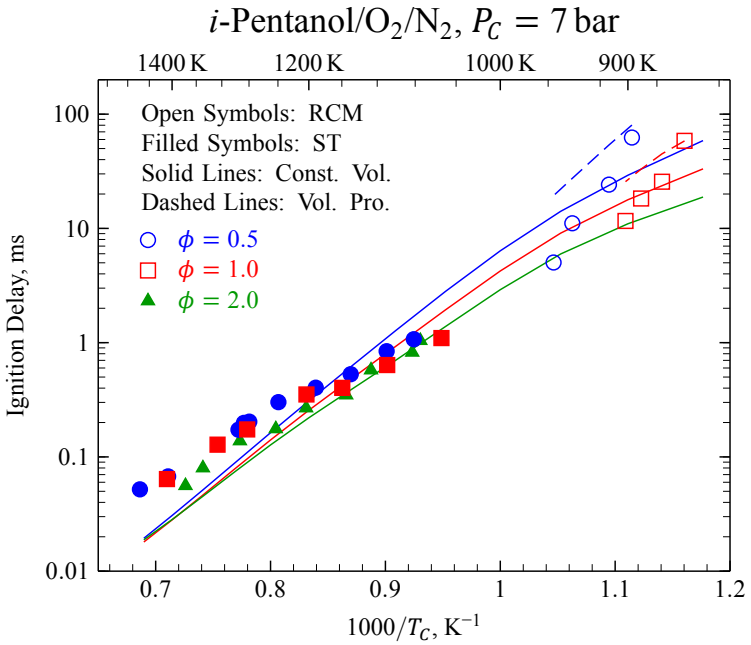

Figure 2: ST and RCM ignition delay times from Tsujimura et al. [4] at 7 atm compared with model predictions by the model from Sarathy et al. [5].

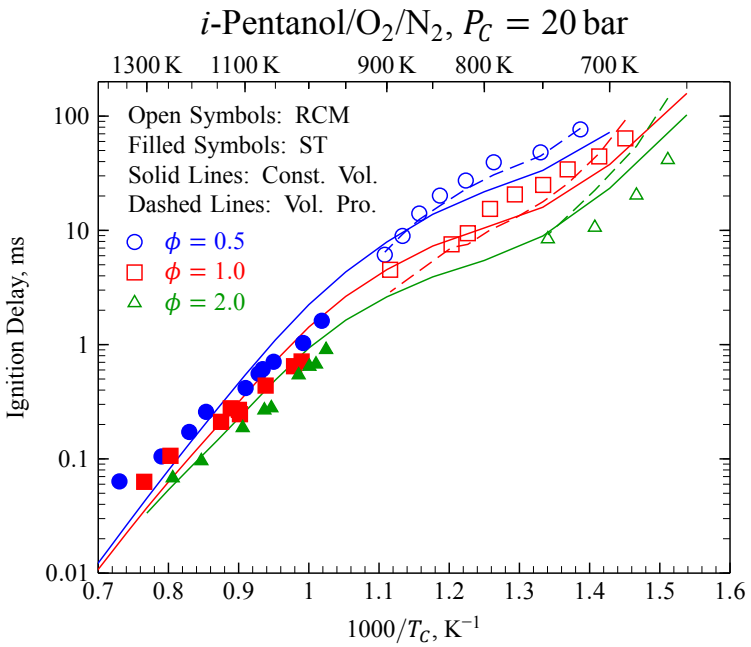

Figure 3: ST and RCM ignition delay times from Tsujimura et al. [4] at 20 atm compared with model predictions by the model from Sarathy et al. [5].

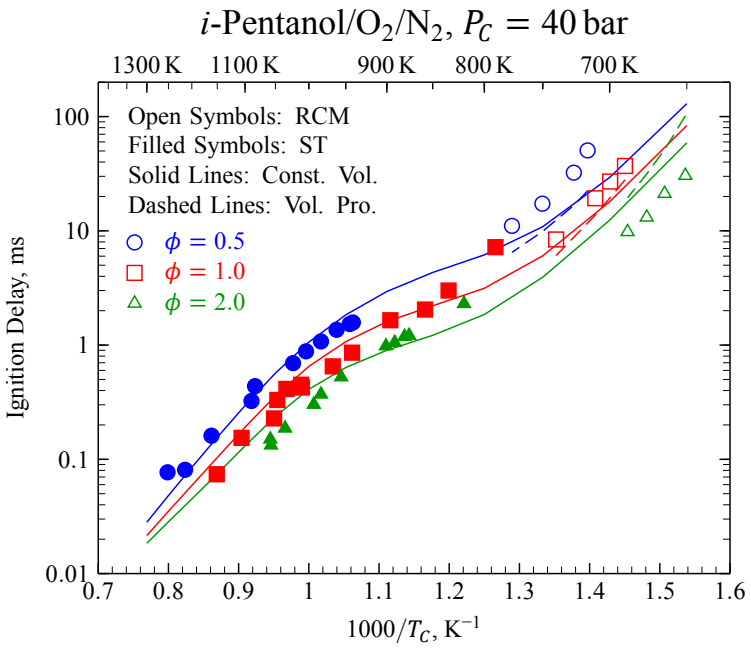

Figure 4: ST and RCM ignition delay times from Sarathy et al. [5] at 40 atm compared with model predictions by the model from Sarathy et al. [5].

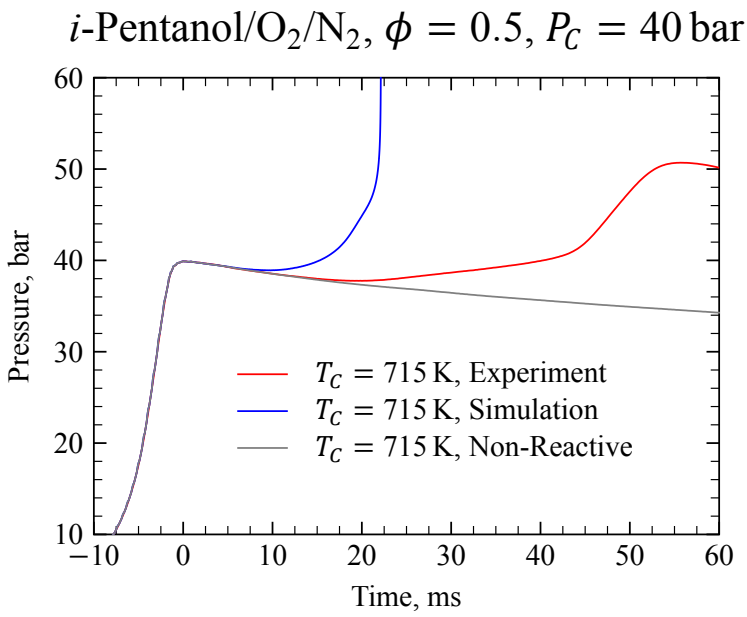

Figure 5: Experimental reactive (red), simulated reactive (blue), and experimental non-reactive (gray) pressure profiles at 40 atm for lean *i*-pentanol/air mixtures.

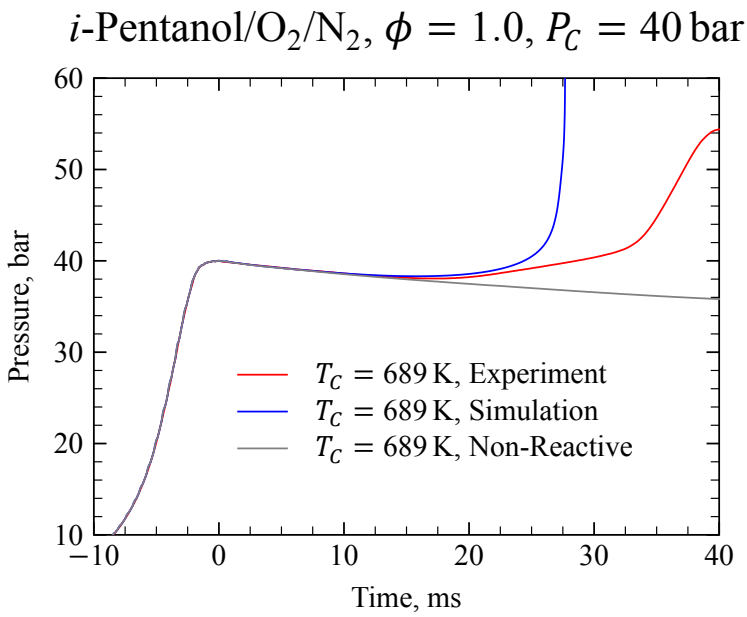

Figure 6: Experimental reactive (red), simulated reactive (blue), and experimental non-reactive (gray) pressure profiles at 40 atm for stoichiometric *i*-pentanol/air mixtures.

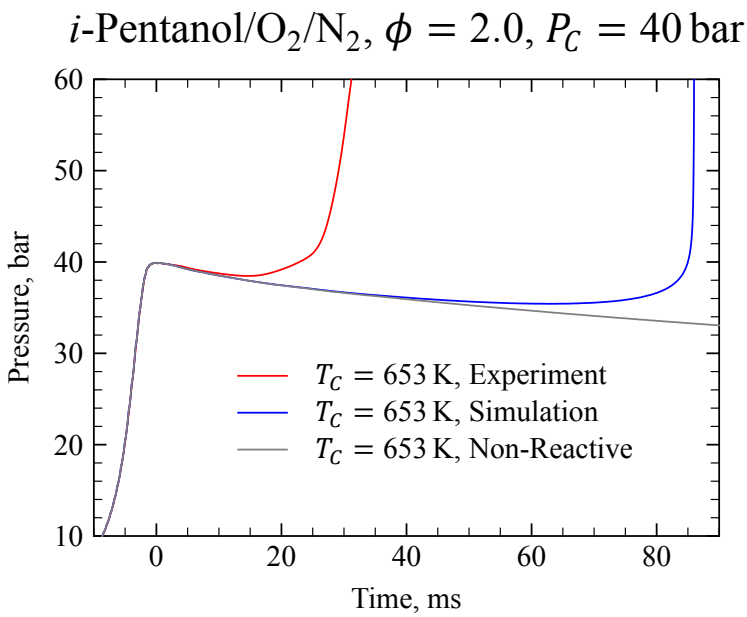

Figure 7: Experimental reactive (red), simulated reactive (blue), and experimental non-reactive (gray) pressure profiles at 40 atm for rich *i*-pentanol/air mixtures.

At 40 atm (Fig. 4), the model is able to reproduce the high-temperature ignition delays fairly well, including capturing the equivalence ratio dependence of the ignition delays. Ignition delay data near 40 atm and temperatures ranging from 651 K to 776 K were also acquired using the RCM. The ignition data in the RCM and ST are in good qualitative agreement, displaying the expected decrease in ignition delay with increasing temperature. The model well predicts the observed trend of decreasing ignition delay time with increasing equivalence ratio, which occurs because a higher fuel concentration results in greater radical production at these conditions. Constant volume and volume history simulations at the 40 atm RCM conditions (Fig. 4) indicate the model can well predict ignition delay times at stoichiometric conditions, but cannot well predict RCM ignition delay data at lean and rich conditions. The difference (i.e., spread) in ignition delay times across various equivalence ratios is similar to that observed for other alcohols in the same facilities (e.g., *n*-butanol at 15 bar [12] and *t*-butanol at 30 bar [13]). The primary issue with the model is its equivalence ratio sensitivity; predicted ignition delay times need to be increased at lean conditions yet decreased at rich conditions, implying that the system's reactivity is controlled by different phenomenon at different equivalence ratios. At these low temperatures the model's reactivity is driven by the overall peroxy reaction sequence, R+O_2=ROO=QOOH(+O_2)=OOQOOH=2OH+products, including the inhibitive direct (i.e., concerted) HO_2 elimination and QOOH decomposition routes. An increase (or decrease) in any reaction rate constant along this reaction sequence will move the reactivity of the system in the same direction at all equivalence ratios. Therefore, we were unable to identify a single reaction rate constant modification that would decrease overall reactivity at lean conditions while increase it at rich conditions.

Representative experimental and simulated pressure profiles for the lean, stoichiometric, and rich conditions are shown in Figs. 5, 6, and 7 respectively, with the profiles shifted so EOC occurs at 0 s. Interestingly, the experimental pressure traces after the induction period do not show a sharp increase in pressure (i.e., heat release is more gradual, similar to two-stage ignition). For the lean case, there is a moderate heat release 25 ms after EOC followed by a larger heat release event, and similar behavior is observed at other equivalence ratios. It is noted that similar heat release prior to

the main ignition event was found in an HCCI engine experiment using *i*-pentanol by Yang et al. [14] and was termed Intermediate Temperature Heat Release (ITHR) in their work.

The pressure profile of the present simulations qualitatively agrees with the experimental data, in that the simulated pressure traces deviate from the non-reactive trace prior to the main ignition event, although the ignition delay itself does not necessarily agree very well. For lean and stoichiometric cases the simulated ignition delay times are fast compared to the data, whereas at rich conditions they are too slow.

0.5 Discussion

The sensitivity of the ignition delay to changes in the reaction rate coefficients is shown in Fig. 8 for a constant volume, adiabatic simulation at 20 atm, 800 K, and for equivalence ratios varying from $\phi = 0.5$ to 2.0. The percent sensitivity is computed by the formula:

$$S = \frac{\tau(2k_i) - \tau(k_i)}{\tau(k_i)} \times 100\,\% \tag{1}$$

where $\tau(2k_i)$ is the ignition delay when the rate coefficient of reaction i is doubled, and $\tau(k_i)$ is the nominal ignition delay. Positive sensitivities therefore represent an increase in the ignition delay when the rate coefficient of reaction i is increased. Both the forward and reverse rates of each reaction are increased simultaneously. Since the reaction 2ho2⇔h2o2+o2 is represented by two sets of A, b, and E_a in the reaction mechanism, both Arrhenius coefficients were simultaneously doubled to give the sensitivity value shown in Fig. 8.

It is seen from Fig. 8 that the most sensitive reaction under these conditions is H-abstraction by OH to form the α-hydroxypentyl radical (ic5h10oh-1). Increasing the rate of abstraction by OH from the α site increases the ignition delay because subsequent reaction of the fuel radical with O_2 leads to the formation of HO_2 and *i*-pentanal, which is an OH terminating pathway. The next most sensitive reaction is H-abstraction by OH to form the γ-hydroxypentyl radical (ic5h10oh-3). The

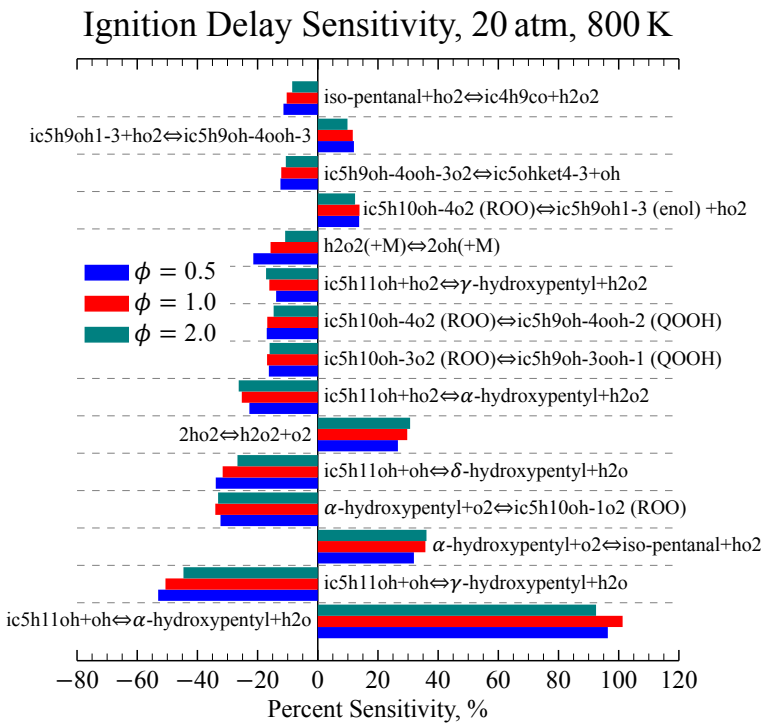

Figure 8: Sensitivity of the ignition delay to changes in the reaction rate coefficients for three equivalence ratios. Initial conditions for constant-volume adiabatic simulations are 800 K and 20 atm.

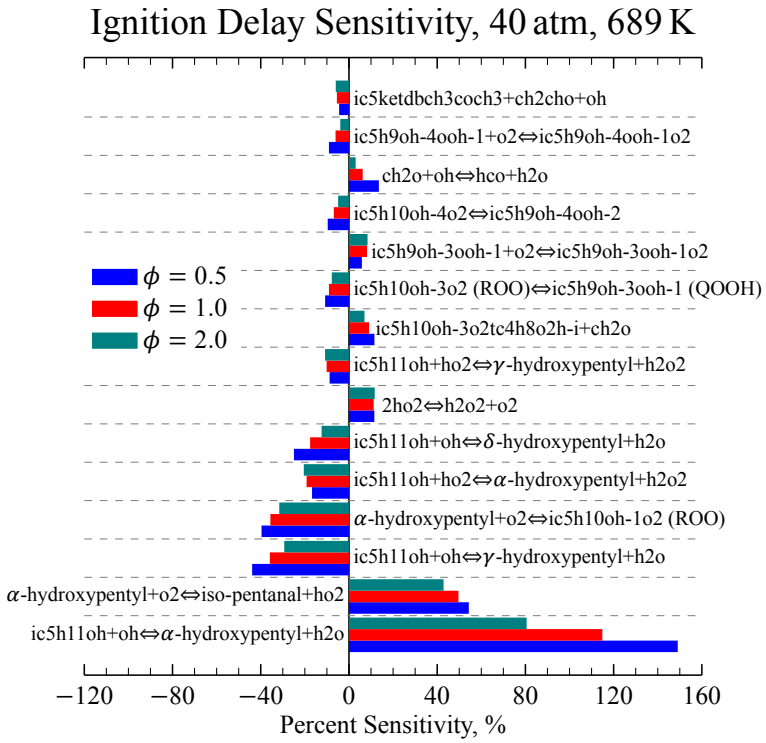

Figure 9: Sensitivity of the ignition delay to changes in the reaction rate coefficients for three equivalence ratios. Initial conditions for constant-volume adiabatic simulations are 689 K and 40 atm.

ignition delay is also sensitive to the rates of isomerization of the ROO radicals formed by the other hydroxypentyl radicals. This indicates that, except for the α radical, the other hydroxypentyl radicals undergo typical low-temperature chain branching reactions. This observation is further corroborated by a reaction path analysis, discussed below. Furthermore, Fig. 8 shows that the ignition delay is also sensitive to some low temperature chain terminating pathways, such as formation of an enol + HO_2 from ROO or QOOH radicals.

A sensitivity analysis of the ignition delay to changes in the reaction rate coefficients for initial conditions of 40 atm and 689 K, for three equivalence ratios, is shown in Fig. 9. As before, positive sensitivity indicates that increasing the rate coefficient of that reaction increases the ignition delay. Similar to the 20 atm sensitivity analysis, the most sensitive reactions are the H-abstractions from the fuel and the subsequent reactions of these initial fuel radicals. However, stronger equivalence ratio dependence of the sensitivity results is seen in Fig. 9 compared to Fig. 8. It is interesting to note that the most sensitive reaction, formation of the α-hydroxypentyl radical through H-abstraction by OH, is nearly twice as sensitive at $\phi = 0.5$ than at $\phi = 2.0$, while most of the other reactions have nearly the same sensitivity for the three equivalence ratios.

In addition, the reaction of formaldehyde and hydroxyl radical to form formyl radical and water is somewhat sensitive, especially for the lean case. The importance of this reaction is demonstrated by the path analysis shown in Fig. 10 (similar results are obtained for a path analysis at 40 atm as at 20 atm). Formaldehyde is a significant product in the decomposition of the β- and γ-hydroxypentyl radicals, as well as the pentoxy radical. Furthermore, the reaction of two hydroperoxyl molecules to form hydrogen peroxide and oxygen molecule is the seventh most sensitive reaction. This reaction is important as it releases the most heat during the ITHR period prior to the main ignition for all three equivalence ratios and because the rapid reaction of the α-hydroxypentyl radical to form *i*-pentanal and hydroperoxyl is important in alcohol combustion. In view of the equivalence ratio dependence shown in Fig. 9, these sensitivity analysis results suggest that it may be possible to adjust multiple reaction rates in the low temperature chain branching pathways to decrease reactivity at lean conditions but increase reactivity at rich conditions, which warrants further investigation.

The main *i*-pentanol reaction pathways after 20 % fuel consumption at 800 K, 20 atm, and for three equivalence ratios are shown in Fig. 10, describing the key low temperature reaction pathways. The percent flux of each reaction path is the contribution of that path to destroying the reactant, integrated up to 20 % fuel consumption. The fuel is mainly consumed by the H atom abstraction at the α site because *i*-pentanol has a weak C-H bond at the α site. As discussed previously, subsequent reactions of α-hydroxypentyl with O_2 generate *i*-pentanal + HO_2, an OH terminating pathway. The other hydroxypentyl radicals tend to add to molecular oxygen and form hydroxyalkylperoxy (ROO) radicals. These radicals are mainly isomerized to hydroxyalkylhydroperoxide (QOOH) or decomposed to enol species by the concerted elimination of HO_2. Approximately 18 % of β-hydroxyalkylperoxy radicals are decomposed to produce *i*-butanal (2-methylpropanal), formaldehyde, and OH radical via ROO isomerization and β-scission reactions by the Waddington mechanism [15, 16]. It is also interesting to note that a similar pathway involving hydrogen transfer from the OH group is important for the γ-ROO (6 %) via a 7-membered transition state ring, which is a reaction sequence we included based on the work of Welz et al. [8].

0.6 Conclusions

New experimental ignition delay data have been collected in an RCM at conditions of 40 atm, $\phi = 0.5$ to 2.0, and temperatures below 800 K. The measured pressure histories showed interesting behavior of slow initial pressure rise prior to a sharp pressure rise indicating overall ignition. This pressure rise may be attributed to the role of the Waddington mechanism in consuming the fuel via the production and recycling of OH radicals during the pre-ignition phase.

An existing model [4] for *i*-pentanol combustion has been updated with newly calculated reaction rate coefficients and newly discovered reaction pathways. The updated model was able to predict the ignition delays measured in the RCM and STs fairly well, although it was unable to reproduce the equivalence ratio sensitivity of the low-temperature RCM ignition delay measurements. The model was also able to qualitatively capture the slow initial pressure rise measured during the RCM

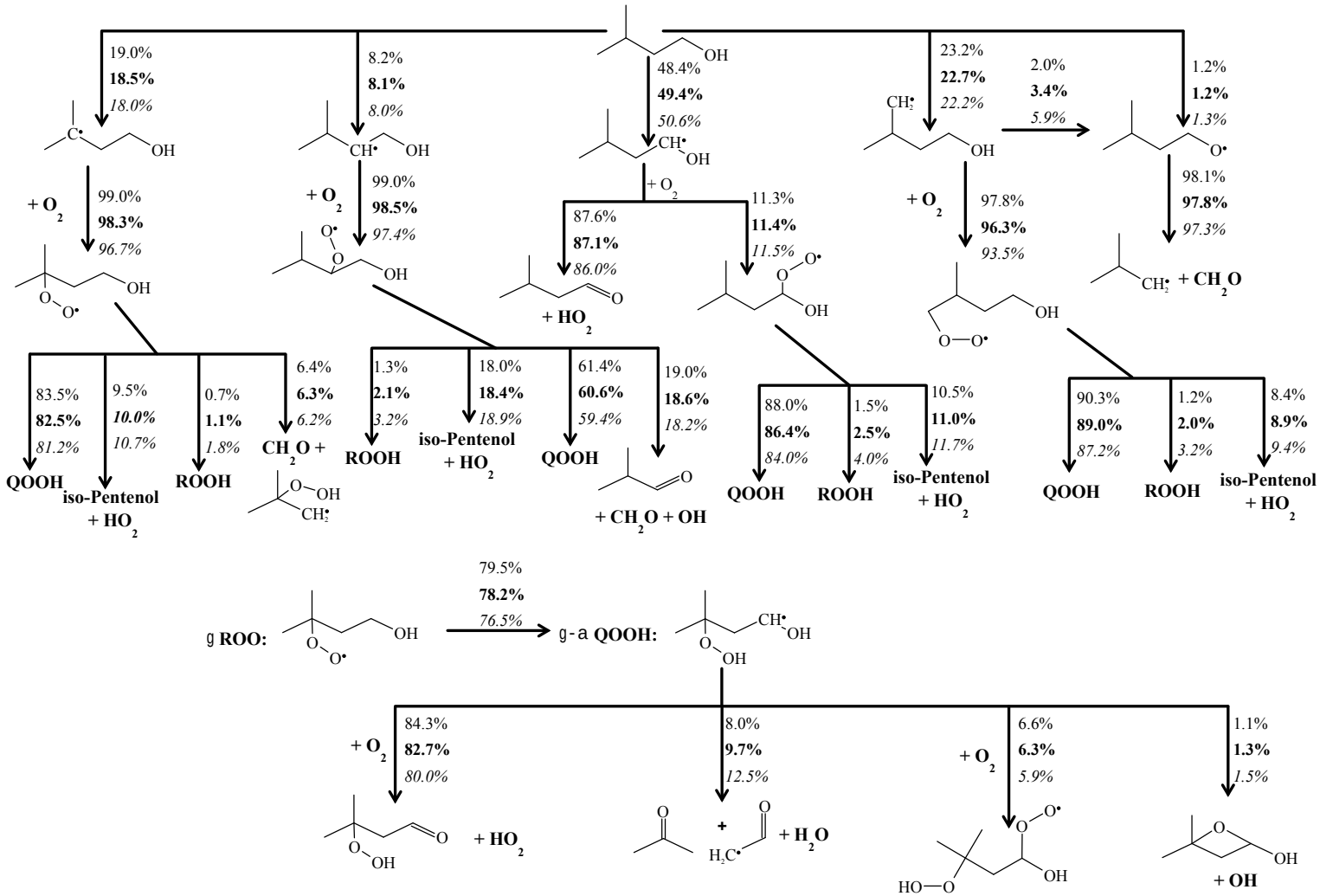

Figure 10: Reaction path analysis for *i*-pentanol at 800 K, 20 atm, and three equivalence ratios, based on constant-volume adiabatic simulations. Plain text: $\phi = 0.5$. Bold text: $\phi = 1.0$. Italic text: $\phi = 2.0$. The flux is integrated up to 20 % fuel consumption.

experiments, although the model was unable to reproduce the quantitative timing of the pressure rise.

Pathway and sensitivity analyses were conducted to understand the important reactions in the decomposition of *i*-pentanol. The most important path for consumption of fuel radicals at low and intermediate temperatures was the reaction of the α-hydroxypentyl radical with O_2 to form *i*-pentanal and HO_2 , a path that does not contribute to the low temperature branching. However, sufficient low temperature chain branching involving the γ and δ fuel radicals occurred in the model that it was able to reasonably reproduce low-temperature ignition and reactivity observed in the experiments. Sensitivity analysis showed that no single reaction can be modified to improve agreement of the model with all of the conditions, and further experimental or computational study is required to identify the cause of the discrepancy in predictions of ignition delay at off-stoichiometric, low-temperature conditions.